SACLANT ASW
RESEARCH CENTRE
MEMORANDUM

HORIZONTAL ARRAY GAIN IN SHALLOW WATER

by

RICHARD KLEMM

15 DECEMBER 1980

NORTH
ATLANTIC
TREATY
ORGANIZATION

LA SPEZIA, ITALY

STI

SACLANTCEN

HORIZONTAL ARRAY GAIN IN SHALLOW WATER

by

Richard Klemm

15 December 1980

This memorandum has been prepared within the SACLANTCEN
Systems Research Division as part of Project 02.

L. F. Whicker

L.F. Whicker
Division Chief

HORIZONTAL ARRAY GAIN IN SHALLOW WATER

R. KLEMM

Saclant ASW Research Centre, Viale San Bartolomeo 400, I-19026 La Spezia, Italy

Abstract. Some results of a comprehensive model study on the use of horizontal hydrophone arrays in shallow water are presented. Well-known signal processing techniques are applied to a shallow-water sound-propagation model in order to investigate the particular influence of shallow-water conditions on the design of spatial receiver structures. A great variety of array processors (optimum, suboptimum, quadratic, linear, adaptive, non-adaptive) are considered. Detection of targets in presence of directive noise sources (e.g. ships) is of particular interest. Some conclusions concerning array processor design for real-time operation are drawn.

Zusammenfassung. Es werden einige Ergebnisse einer umfassenden Modellstudie über die Anwendung von horizontalen Hydrophongruppen in flachem Wasser präsentiert. Bekannte Signalverarbeitungsverfahren werden auf ein Flachwasser-Schallausbreitungsmodell angewandt, um den besonderen Einfluss der Flachwasserbedingungen auf die Konstruktion von räumlichen Empfängerstrukturen herauszufinden. Eine grosse Anzahl von Array-Prozessoren (optimal, suboptimal, quadratisch, linear, adaptiv, nicht adaptiv) werden diskutiert. Zielsignalentdeckung in Gegenwart gerichteter Störquellen (z.B. Schiffe) ist von besonderem Interesse. Es werden einige Schlussfolgerungen bezüglich der Konstruktion von Array-Prozessoren für Echtzeitbetrieb gezogen.

Résumé. On présente quelques résultats d'une étude d'ensemble des utilisations d'antennes horizontales en eaux peu profondes. En appliquant des techniques bien connues de traitement du signal à un modèle de propagation du son en eau peu profonde, on examine l'influence particulière des conditions propres aux faibles profondeurs sur la conception de la partie spaciale des structures réceptrices. Une grande variété de processeurs sont pris en considération (optimaux, suboptimaux, quadratiques, linéaires, adaptatifs, non adaptatifs). La détection d'objectifs dans un champ de bruit directif (par exemple en provenance de navires) présente un intérêt tout particulier. Pour finir on tire quelques conclusions quant à la conception de processeurs destinés au traitement en temps réel des signaux des antennes.

Keywords. Array processor, nullsteering, adaptive beamforming, normal modes, shallow water.

1. Introduction

The following investigation has been done in order to find out which kind of spatial signal processing should be applied to linear horizontal hydrophone arrays in shallow water. The theory of optimum arrays has been treated repeatedly in literature, e.g. [1, 2, 3, 4, 5]. Many other papers, e.g. [6], are concerned with suboptimum adaptive approaches to optimum array processing, in particular, by replacing the crucial inversion of the noise covariance matrix contained in all adaptive array processors by some algorithms for minimizing the noise, e.g. LMS-algorithm. The same basic ideas have been used for adaptive clutter suppression in pulse radars [7, 8]. In the major part of the literature on adaptive beamforming only linear processors have been considered. This means that the signal is supposed to be a plane coherent wave. In many applications, e.g. radar and small sonar arrays, this assumption is justified. In this paper simplification of processor structures is made under the constraint that the spatial characteristics of shallow-water sound-propagation are taken

into account. Target detection in presence of point shaped interference sources is of special interest.

Throughout the paper the narrow band case is considered. The results can be easily extended to broadband systems by carrying out the spatial part of the processing in sufficiently narrow subbands and summing the spectral signal components in an appropriate way [4, 9].

2. Signal and noise model

It is the intention of this paper to compare the gain of different array processors in shallow water by means of a normal mode sound propagation model. The spatial gain of any quadratic or linear array processor is given by the spatial covariance matrices of signal and noise. Therefore, one has to derive the covariance matrices of signal and interference from the outputs of the given computer model The SNAP-model [10] used in this investigation computes a set of M modal horizontal wave numbers k_n and modal amplitudes A_n for a set of environmental input parameters, such as receiver-source geometry, frequency and channel parameters. The sound pressure of a mono-chromatic source received at distance r can be written as

$$p(r, z, z_0, t) = e^{-j\omega t} \sum_{n=1}^{M} A_n e^{jk_n r}. \qquad (2.1)$$

The modal amplitudes are

$$A_n = a \frac{\omega \rho^2}{H} \sqrt{\frac{1}{8\pi r}} \frac{u_n(z_0) u_n(z)}{\sqrt{k_n}} e^{-\alpha_n r - \pi/4}, \quad (2.2)$$

where a is the source strength, $\omega = 2\pi f$, ρ = water density, H = water depth, r = range, z = receiver depth, z_0 = source depth, α_n = modal attenuation coefficient, $u_n(z)$ = normal mode function [11]. Each of the wave components in (2.1) is associated with a modal vertical incident angle γ_n defined by

$$\cos \gamma_n = \frac{k_n}{k_0}, \qquad k_0 = \frac{\omega}{c(z)},$$

$c(z)$ being the sound velocity at receiver depth.

In order to introduce the geometry of a linear horizontal array with uniform spacing d we have to replace the range r in (2.1, 2.2) by

$$r = r_0 + d_i,$$

$$d_i = di \cos \beta, \quad i = 0, \ldots, N-1, \qquad (2.3)$$

N being the number of sensors and β the angle between the array axis and the horizontal direction of wave propagation. The output signal at the ith sensor is consequently

$$x_i = C_i e^{-j\omega t} \sum_{n=1}^{M} A_n(i) e^{jk_n(r_0 + d_i)}, \qquad (2.4)$$

where the C_i are the complex gain factors of individual channels. We assume in the following that $C_i = 1 \ \forall i$. The elements of the covariance matrix $\mathbf{P}$ of received signals contains the elements

$$\rho_{il} = E\{x_i x_l^*\}$$

$$= \sum_{n=1}^{M} A_n(i) e^{jk_n(r_0 + d_i)} \sum_{m=1}^{M} A_m(l) e^{-jk_m(r_0 + d_i)}$$

$$= \sum_{n=1}^{M} A_n(i) A_n(l) e^{jk_n(d_i - d_l)}$$

$$+ \sum_{\substack{n=1 \ m=1 \\ n \neq m}}^{M} \sum^{M} A_n(i) A_m(l)$$

$$\times e^{j[(k_n - k_m) r_0 + k_n d_i - k_m d_l]}. \qquad (2.5)$$

The first term of (2.5) is the incoherent summation of the radiation in all modes. The second expression is the mode interference term.

So far the model is entirely deterministic. Let us introduce now some randomness due to channel fluctuations. It has been shown by several authors [11, 12] that scattering by randomly varying boundaries causes the individual modal components of the received signals to be random in amplitude and phase. This results in a slight increase of modal attenuation coefficients α_n in (2.2) and a decrease of the mode interference term in (2.5). The increase of the α_n is taken into account by the SNAP model [10]. The interference term we suppose to be zero in the following investigation by several reasons. First of all, there

may be some additional uncertainty due to volume scattering and other internal fluctuations of the medium. Volume scattering has been modelled in [17] by an independent modal phase, thus causing modes to be uncorrelated among each other. Consequently, wavefronts of signal and interference become random. The assumption of random signal wavefronts is an essential feature of this paper and different from most other publications in that field. Finally, dropping the interference term in (2.5) yields considerable saving in arithmetic operations.

In the following, signal and interference are described by covariance matrices $\mathbf{P}$ and $\mathbf{Q}_I$ with elements of the form

$$\rho_{il} = \sum_{n=1}^{M} A_n(i)A_n(l)\, e^{jk_n(d_i-d_l)}. \qquad (2.6)$$

Notice that for broadside direction ($\beta = 90°$) we get $d_i = 0 \;\forall i$. Inserting this in (2.6) and (2.2) the elements of $\mathbf{P}$ and $\mathbf{Q}_I$ become independent of i and l:

$$\rho_{il} = \sum_{n=1}^{M} A_n^2(r_0).$$

This means $\mathbf{P}$ and $\mathbf{Q}_I$ have rank 1. In other words, wavefronts due to sources at broadside direction appear to be coherent because of the rotational symmetry of line arrays.

For the simulations presented below, the parameters A_n and k_n have been obtained from the normal mode program SNAP [10]. A typical example is shown in Fig. 1a and 1b where the logarithms of the modal amplitudes A_n are plotted versus the vertical angle of arrival $\gamma_n = \arc\cos(k_n/k_0)$. Fig. 1a shows the case of an interference located at 1 km range and 2 m depth. Fig. 1b shows the energy distribution of the target (10 km range, 50 m depth). Array depth is 50 m, frequency 800 Hz, an isovelocity sound speed profile is assumed. This example is used in all following investigations. In addition spatial white noise independent of interference and signal is assumed in order to model roughly non-directive kinds of noise (ambient, surface, flow, receiver,
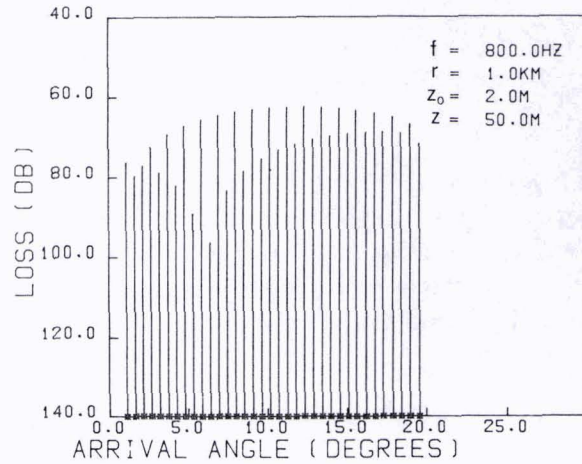
Fig. 1a. Vertical energy distribution of noise sources.
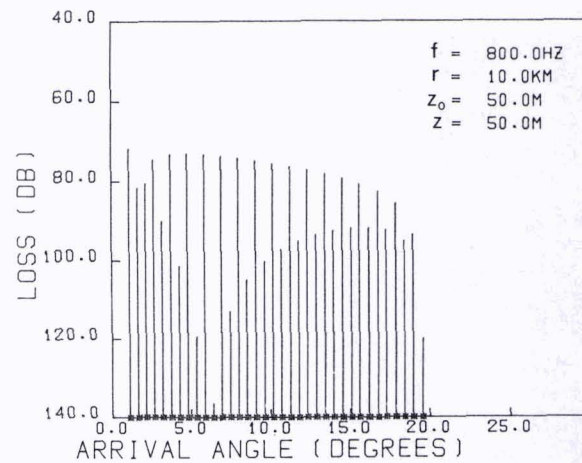
Fig. 1b. Vertical energy distribution of target.

reverbs). Now the covariance matrix of interference and noise is $\mathbf{Q} = \mathbf{Q}_I + P_w\mathbf{I}$ where P_w is the white noise power. $\mathbf{Q}$ is now positive definite even for broadside interference.

3. The Optimum Quadratic Processor (OQP)

Quadratic processors are represented in Hermitian form by

$$\psi \equiv x^*\mathbf{K}x \quad \eta \quad \begin{array}{ll} > & \text{target + noise,} \\ & \text{decision} \\ < & \text{noise alone.} \end{array} \qquad (3.1)$$

The processor matrix **K** can be optimized in the likelihood ratio sense if both signal and noise are gaussian. In this case **K** is defined by [4]

$$\mathbf{K} = \mathbf{Q}^{-1} - (\mathbf{P} + \mathbf{Q})^{-1}, \tag{3.2}$$

where $\mathbf{Q} = E\{\boldsymbol{nn}^*\}$ and $\mathbf{P} = E\{\boldsymbol{ss}^*\}$ are the covariance matrices of noise and signal respectively. Equation (3.2) is quite difficult to implement and, furthermore, the absolute power levels of signal and noise must be known a priori. The choice

$$\mathbf{K} = \mathbf{Q}^{-1}\mathbf{P}\mathbf{Q}^{-1} \tag{3.3}$$

is optimum in the signal-to-noise ratio sense for non-gaussian signal and gaussian noise [4]. Any change in the absolute power level of $\boldsymbol{n}$ or $\boldsymbol{s}$ will just result in a proportional change of the detection threshold η. The gain of any quadratic processor has been defined in [5] to be the ratio of detection index to the input signal-to-noise ratio of the array. The average input signal power is $P_s = \mathrm{tr}(\mathbf{P})$ and the noise power $P_n = \mathrm{tr}(\mathbf{Q})$. The detec-

tion index is defined as [4]

$$D = \frac{E\{\psi \mid \sigma + \nu\} - E\{\psi \mid \nu\}}{[E\{\psi^2 \mid \nu\} - E^2\{\psi \mid \nu\}]^{1/2}}, \tag{3.4}$$

where ν means noise and $\sigma + \nu$ means signal + noise.

For gaussian noise the gain of a quadratic processor becomes [4]

$$G = \frac{\mathrm{tr}(\mathbf{H}^*\mathbf{P}\mathbf{H}) \cdot P_n}{\sqrt{\mathrm{tr}[(\mathbf{H}^*\mathbf{Q}\mathbf{H})^2]} \cdot P_s}. \tag{3.5}$$

H is achieved by factorization of the positive definite processor matrix $\mathbf{K} = \mathbf{H}^*\mathbf{H}$. In the optimum case (3.3) one gets

$$\mathbf{K} = \mathbf{Q}^{-1}\mathbf{F}\mathbf{F}^*\mathbf{Q}^{-1}$$

where $\mathbf{Q}^{-1}$ represents noise suppression and **F** is a generalized matched filter.

Fig. 2 shows a typical numerical example. Two interfering point sources are assumed to be at 0° and 90° with an interference-to-noise ratio of
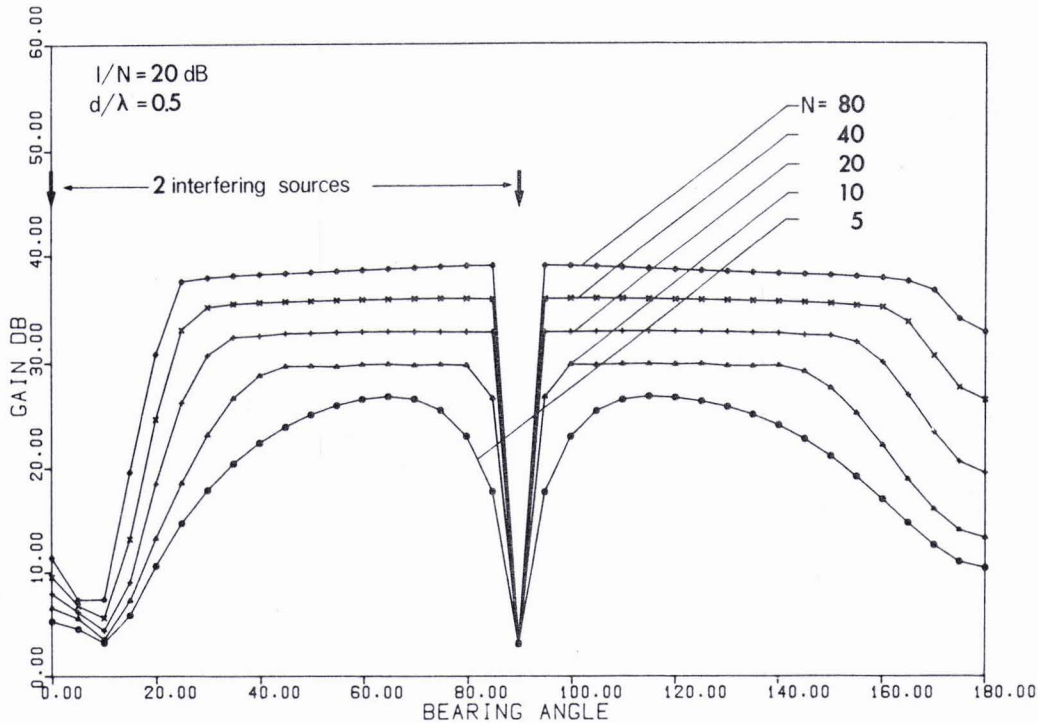

Fig. 2. Gain achieved by optimum quadratic processing.

20 dB each. Different curves show the gain in signal-to-interference ratio for different numbers of sensors N plotted versus the bearing of the target. The spatial spread of the noise as appearing in the horizontal can be recognized by comparing the minima at the locations of the interfering sources. At broadside (90°) there is no spread whereas at endfire (0°) the interference appears to be distributed over about 20°. The plane areas in the middle show the white noise limitation. The minimum on the right is a periodical repetition of the minimum at 0° due to the field sampling ($d/\lambda =$ 0.5).

The OQP is not very useful for real-time applications except for very small arrays because it requires about $2N^3$ complex multiplications. In addition numerical problems will arise for large N if the interference-to-noise ratio is high. In the following the OQP is used for comparison with suboptimum systems.

4. The Optimum Linear Processor (OLP)

Linear processors are described by a scalar product

$$\psi \equiv \mathrm{Re}\{x^*h\} \quad \begin{matrix} > \\ \eta \\ < \end{matrix} \quad \begin{matrix} \text{target + noise,} \\ \text{for decision} \\ \text{noise alone.} \end{matrix} \quad (4.1)$$

The linear spatial filter h is usually a product of a noise suppression matrix $\mathbf{W}$ and a beamformer b:

$$h = \mathbf{W}b. \quad (4.2)$$

The gain in signal-to-interference ratio achieved by any h is

$$G = \frac{h^*\mathbf{P}h}{h^*\mathbf{Q}h} \frac{P_n}{P_s}. \quad (4.3)$$

Optimization of h in the maximum likelihood or maximum signal-to-noise ratio sense yields $\mathbf{W} = \mathbf{Q}^{-1}$ [2, 3] if the signal is deterministic. The optimum linear processor $h = \mathbf{Q}^{-1}b$ has been approximated by an LMS-algorithm by Widrow [6] and many others. Applying the optimum linear pro-

cessor to the signal and noise models described above yields gain curves as shown in Fig. 3. A comparison between OQP and OLP is made for $N = 20$ and $N = 160$. For the short array there is obviously no significant difference between linear and quadratic processing. For large arrays (e.g. $N = 160$) some dB of gain are lost for bearing angles different from broadside. The reason is that the beamformer of the OLP is mismatched to the spread signal (except for broadside). This does not matter as long as the beamwidth is larger than or equal to the signal spread. If the beamwidth becomes too narrow signal energy is lost, thus causing loss in gain.

It can be further noticed that even the gain achieved by the OQP decreases slightly for bearings different from broadside. This is the loss due to the assumption of uncorrelated modes. As pointed out in Section 2, any source at broadside causes a coherent plane wave. If modes are uncorrelated the wavefront appears to be more and more random for angles different from broadside.

5. Shading

The well-known shading methods are described by the linear processor (4.1) if $\mathbf{W}$ is chosen to be a diagonal matrix containing the shading coefficients w_i as diagonal elements. Basically, shading coefficients can be optimized so that the signal-to-noise ratio becomes maximum, i.e.

$$\max_h h^*\mathbf{P}h/h^*\mathbf{Q}h.$$

However, this leads to the cumbersome procedure of solving an eigenvalue problem of the kind $(\mathbf{P} - \lambda \mathbf{Q})h = 0$ where the eigenvector corresponding to the maximum eigenvalue is the solution.

In the following only a shading-function of the form

$$W_i = 0.5 - 0.5 \cos(2\pi(i - 0.5)/N),$$
$$i = 1, \ldots, N, \quad N \text{ even} \quad (5.1)$$

is considered. A comparison of the cos-shading processor with the OQP is presented in Fig. 4. It
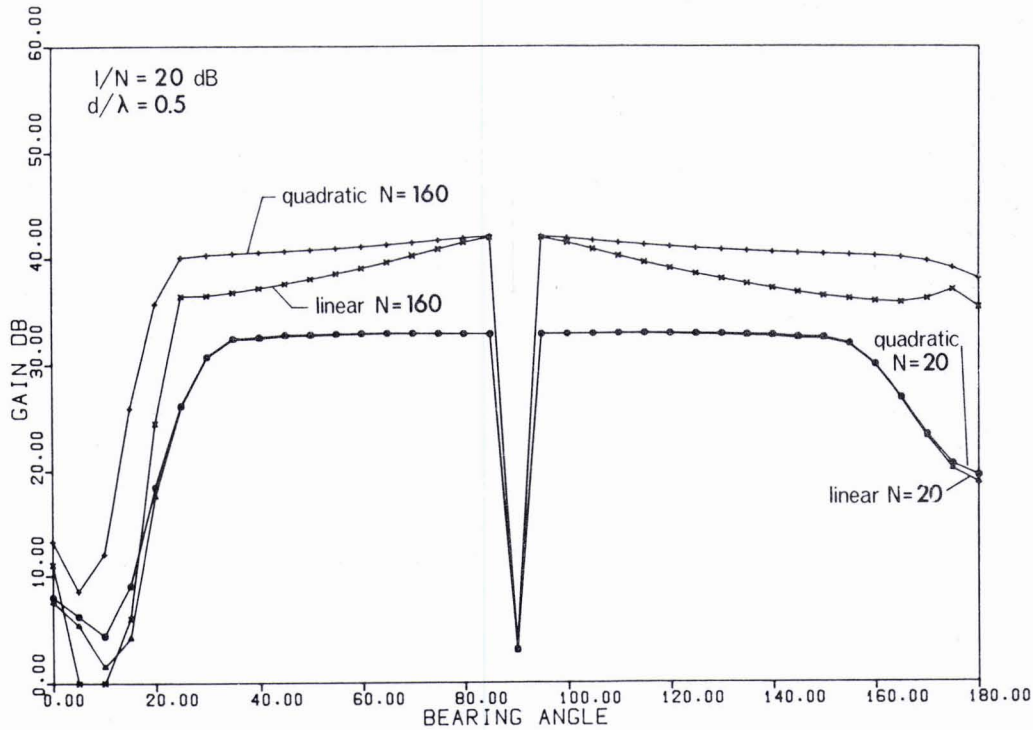
Fig. 3. Optimum quadratic and optimum linear processing.

can be seen that there is always a certain plane part in the gain curves (white noise limitation) where the gain is just 3 dB below the OQP-gain. For small arrays (e.g. $N = 20$), however, the main beam becomes very broad so that the main lobe interference becomes unbearable. However, for a certain array length ($N = 80$) a reasonable approximation of the OQP-performance is achieved. The minimum on the right can be removed by using a spacing smaller than $d/\lambda = 0.5$ (but the same aperture). For larger apertures the beam becomes too narrow so that signal energy is lost. Other kinds of shading could be considered as well, yielding different ratios of sidelobe level and beamwidth and thus leading to another optimum array length.

6. Nullsteering methods

In some cases the direction of a noise source is known a priori (for instance, the direction of a ship

towing the array). In such cases suppression of the directive noise can be performed by steering nulls either of the array pattern or of the individual sensor patterns in the direction of the interfering source. A null in the array pattern is achieved by choosing the noise suppression matrix in (4.2) to be

$$\mathbf{W} = \mathbf{I} - \frac{cc^*}{c^*c}, \tag{6.1}$$

if only one null is formed. The vector describes the direction of the interference. Any product $\mathbf{W}a$ (a being an arbitrary vector) gives a projection of a on a subspace orthogonal to c. The method (6.1) has been used in [15] for suppression of interference. If there are more than one interfering sources is replaced by a matrix $\mathbf{C}$ containing different vectors as columns so that

$$\mathbf{W} = \mathbf{I} - \mathbf{C}(\mathbf{C}^*\mathbf{C})^{-1}\mathbf{C}^*. \tag{6.2}$$

Notice that $\mathbf{WC} = \mathbf{O}$ if the rank of $\mathbf{C}$ is smaller than N and $\mathbf{W} = \mathbf{O}$ if the rank of C is equal to N, i.e. the
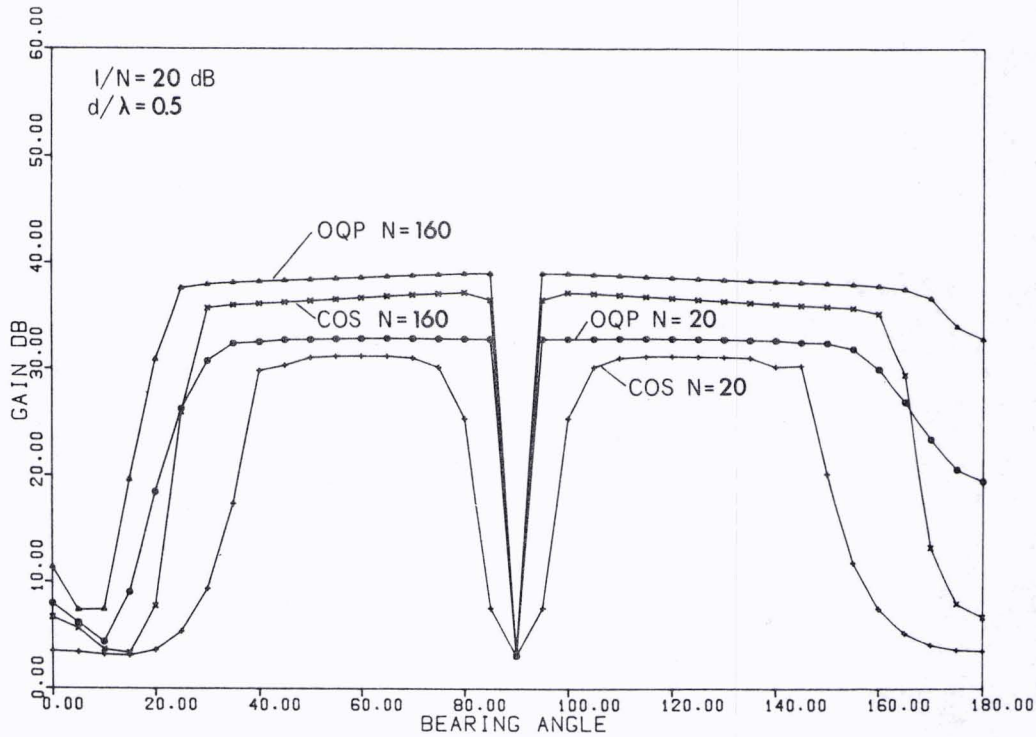
Fig. 4. Comparison of OQP and COS-shading.

array becomes blind for any direction. Dipole or cardioid patterns are obtained by appropriate combination of adjacent sensors. The corresponding noise suppression matrix is given by

$$
\mathbf{W} = \begin{pmatrix} 1 & & & & 0 \\ -c_1 & 1 & & & \\ & -c_1 & \cdot & & \\ & & \cdot & \cdot & \\ & & & \cdot & \cdot \\ 0 & & & -c_1 & 1 \end{pmatrix} \tag{6.3}
$$

where c_1 denotes the phase factor corresponding to the interference direction.

Fig. 5 shows a comparison of methods (6.1) and (6.3) with the OQP for a short array ($N = 20$). There is only one interfering source at endfire. It can be seen that the broad nulls of dipole sensors cope quite well with the spatial spread of the signal. Very good coincidence with the OQP is achieved over a broad area. The deviation between OQP and dipole processor gain around 180° is due to the fact that there is another null in the dipole pattern opposite to the interference direction. This is avoided by choosing a smaller spacing, e.g. $d/\lambda = 0.3$, thus forming some kind of cardioid pattern. A null in the array pattern as described by (6.1) is obviously too narrow for adequate suppression of the spread signal.

7. Pre-transform array processors

The array processors treated in this section differ from the previous one in that the received signals are first pre-transformed

$$
y = \mathbf{T}x = \mathbf{T}(s + n) \tag{7.1}
$$

where $\mathbf{T}$ is an $L \times N$ matrix. The covariance
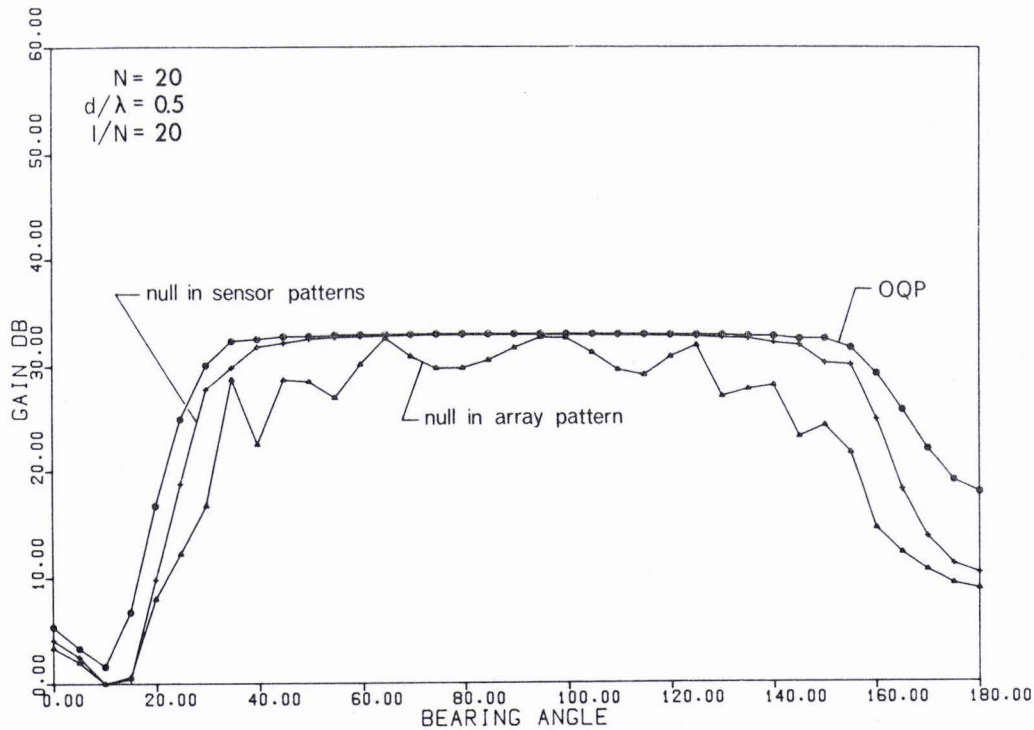
Fig. 5. Nullsteering methods.

matrices of signal and noise become

$$S = E\{Tss^*T^*\} = TPT^*,$$
$$N = E\{Tnn^*T^*\} = TQT^*. \tag{7.2}$$

The pre-transform should be chosen so that
  • $L \ll N$ in order to spare arithmetic operations,
  • L is sufficiently large for adaptive suppression of interference, i.e. $L >$ number of interfering sources,
  • no signal energy is lost.

The third requirement can be met by steering one or more beams in the hypothetical target direction. In general, the pre-transform has the form

$$T \equiv \begin{pmatrix} \text{beamforming} \\ \cdots \\ \text{noise estimation} \end{pmatrix}.$$

So the main difference between pre-transform and the other processors discussed before is that the order of beamforming and noise suppression is changed. Typical pre-transforms are

$$T \equiv \begin{pmatrix} 1 & & & & b^* & & 0 \\ & 1 & & & & & \\ & & \ddots & & & & \\ 0 & & & 1 & 0 \cdots 0 \end{pmatrix}$$

or

$$T \equiv \begin{pmatrix} b_1^* \\ b_2^* \\ \vdots \\ b^* \end{pmatrix} \tag{7.4}$$

the first of them using auxiliary sensors, the second auxiliary beams for noise estimation. The auxiliary sensor concept has been investigated in a modified form by Owsley [4]. The quadratic processor after the pre-transform becomes

$$l \equiv x^*T^*N^{-1}SN^{-1}Tx \tag{7.5}$$

and the linear processor

$$l \equiv \mathrm{Re}\,\{x^*T^*N^{-1}Tb\}. \tag{7.6}$$

The gain of the quadratic processor is again

$$G = \frac{\mathrm{tr}(F^*SF)}{\sqrt{\mathrm{tr}[(F^*NF)^2]}} \cdot \frac{P_n}{P_s} \tag{7.7}$$

where F is the spatial filter after the pre-transform. The optimum F is

$$F = N^{-1}H, \tag{7.8}$$

where H is obtained by factorization $S = HH^*$. The gain of the linear processor becomes

$$\frac{e_b^*N^{-1}SN^{-1}e_b}{e_b^*N^{-1}e_b} \cdot \frac{P_n}{P_s} \tag{7.9}$$

where e_b is a unity vector selecting just that beam which points in the hypothetical target direction (if there is more than one).

A numerical example for the gain of the optimum quadratic pre-transform processor (7.7, 7.8)

is shown in Fig. 6 for two array lengths ($N = 20$, 160). A multi-beam processor (MBP, (7.4), right side) with 5 orthogonal beams centered around the target is compared with the OQP and an auxiliary element type processor (ASP, left side of (7.6)). The MBP is obviously a very good approximation of the OQP (about 1 dB less) for short and large arrays as well. The performance of the ASP is somewhat inferior. In particular, it shows still some side-lobe ripple. The reason is that the interference-to-noise ratio in the beam changes while moving in bearing, whereas the I/N in the auxiliary sensor is always constant. If, however, the beams of an MBP are chosen so that the neighbouring beams overlap each other orthogonally the interference-to-noise ratio in all beams is almost equal for all target-directions, i.e. the ratio of interference-to-noise ratios between beams is almost independent on bearing which causes quite smooth gain curves. It is obvious from Fig. 3 that the ASP will yield some loss in gain for
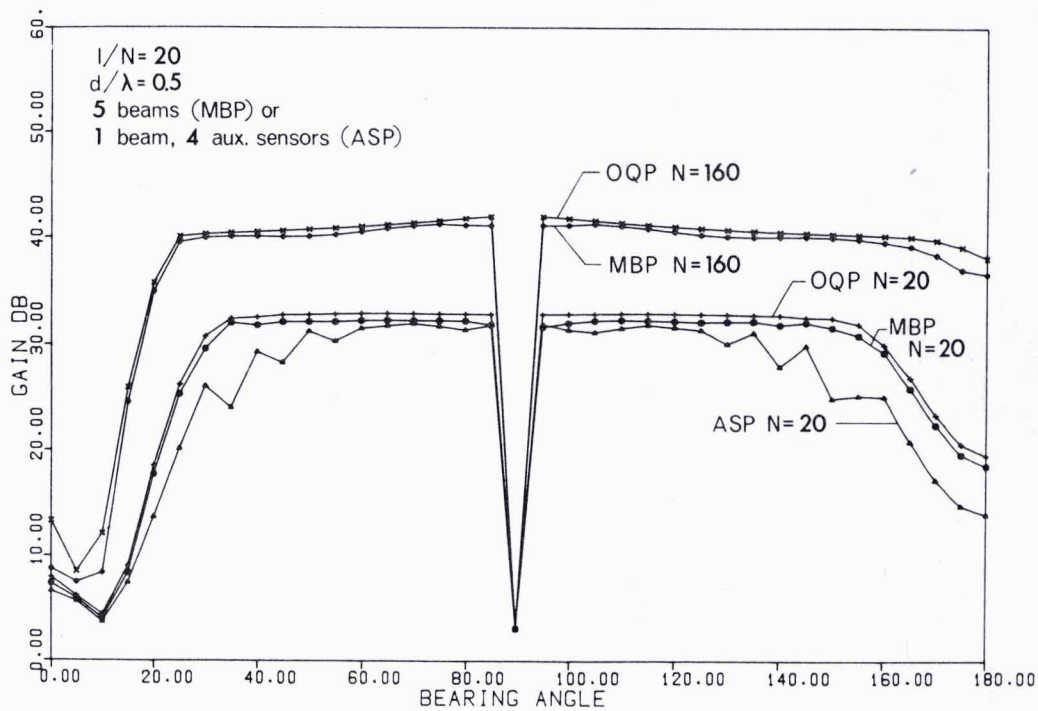

Fig. 6. Adaptive noise cancellers.

large arrays because there is only one beam in the pre-transform. So the ASP behaves like a linear processor.

A comparison between linear (LP) and quadratic (QP) processing is shown in Fig. 7 for different values of N. As is already known from Fig. 3, there is almost no difference between QP and LP for short arrays ($N = 20$). The difference becomes significant for $N > 40$. For very large arrays ($N = 160$) the gain of the linear processor may become even smaller than the gain of much smaller arrays (compare with $N = 40$). A comparison with Fig. 3 shows that the linear pre-transform processors are more sensitive to a mismatch between beam and signal than the OLP. Only at broadside where the signal is a plane wave do quadratic and linear processors yield the same gain.

8. Suboptimum quadratic pre-transform processors

In practice the matrices $\mathbf{Q}$ and $\mathbf{N}$ are obtained by some estimation procedure (adaptation to noise field). The signal covariance matrices $\mathbf{P}$ or $\mathbf{S}$ which are needed for calculation of the generalized beamformer have to be known a priori, e.g. by running a modelling program. This is a tedious procedure, in particular because the results are range dependent. It is, therefore, desirable to find a simple quadratic beamforming system that does not depend on the individual channel characteristics and, particularly, not on range. One possibility is to assume the signal energy to be uniformly distributed over a certain angle interval, whose width depends on bearing. The covariance
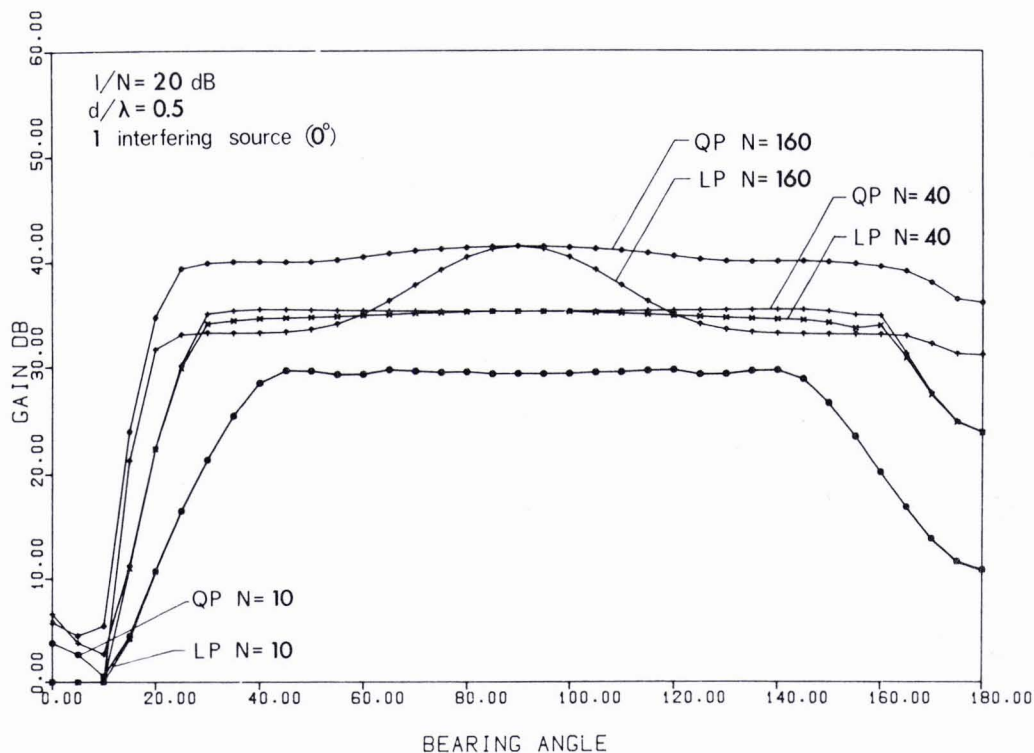

Fig. 7. Quadratic vs linear multi-beam processing.

matrix $\mathbf{R}$ for this signal model contains the values

$$\rho_{il} = \sin c(a_0(i-l)) \exp(jb_0(i-l)), \qquad (8.1)$$

where

$$a_0 = d\frac{\pi}{\lambda} u_0 \cos \beta \quad \text{and} \quad b_0 = dk \cos \beta,$$

u_0 being the interval width at endfire and $k = 2\pi/\lambda$. The beamformer matrix $\mathbf{H}$ is again obtained by factorization $\mathbf{R} = \mathbf{H}^*\mathbf{H}$. Notice that $\mathbf{R}$ becomes singular for broadside $(\beta = 90°)$; here the factorization leads to the linear beamformer which is in fact optimum for broadside.

Another even simpler quadratic beamformer is given by summation of the squared beam outputs of the MBP.

Both methods just described are compared with the optimum quadratic MBP and the linear one in Fig. 8. The $\sin c$ beamformer (8.1) gives an approximation to the MBP by about 2 dB loss. Incoherent summation of beam outputs is almost

identical to the $\sin c$ beamformer except for the area around broadside where even the linear processor is better. This is because around broadside the signal spread is so small that only one beam of the MBP carries signal energy whereas the other ones contribute only noise.

As a result we find a rule of thumb: Provide a certain number of orthogonally overlapping beams for cancellation of interference but adjust the number of beams used for incoherent beam integration to the spread of the signal, i.e. to the bearing. In particular, at broadside only the output of that beam which points at broadside direction should be used.

9. Inclusion of signal in adaptation

In passive systems no signal-free estimate of the noise covariance matrix may be obtained because
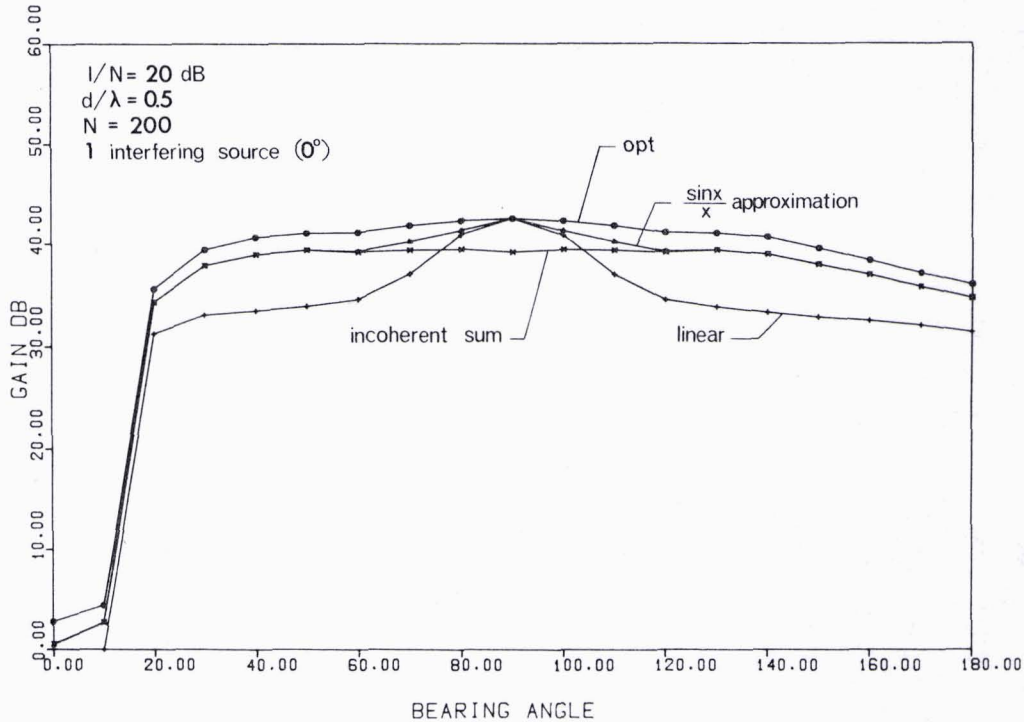

Fig. 8. Comparison of quadratic multi-beam processing.

the signal cannot be switched off. Therefore the matrix in (7.2) and hence (7.7, 7.9) contain signal and noise which leads to serious decrease of the gain achieved by the adaptive processors (7.5, 7.6) if the beamformers **H** or **b** are not perfectly matched to the signal [9]. A well-known technique to overcome this problem is a so-called constrained adaptive processor (e.g. [4]). A simple realization of constrained processors is an auxiliary element processor using dipoles with the null being steered in the target direction for signal-free noise estimation, i.e. choosing the pre-transform to be

$$\mathbf{T} \equiv \begin{pmatrix} & & & b^* & & \\ 1 & -b_1^* & & & & \\ & 1 & -b_1^* & & & 0 \\ & & & \cdot & & \\ 0 & & & 1 & -b_1^* & 0 \cdots 0 \end{pmatrix} \quad (9.1)$$

However, complete signal suppression is achieved only if the signal is a plane wave. In our case this happens only for broadside. In addition broadside is the only direction where a beamformer can be perfectly matched. For directions other than broadside a certain decrease in gain can be expected. Fig. 9 shows some typical gain curves plotted for different target ranges. It is seen that a reasonable approximation to the OQP-performance is achieved only for broadside.

10. Conclusions

Some theoretical results concerning the gain of horizontal linear arrays in shallow water have been presented. Comparison of different methods for suppression of directive noise sources under shallow water propagation conditions have been discussed. The major conclusions are listed as follows:
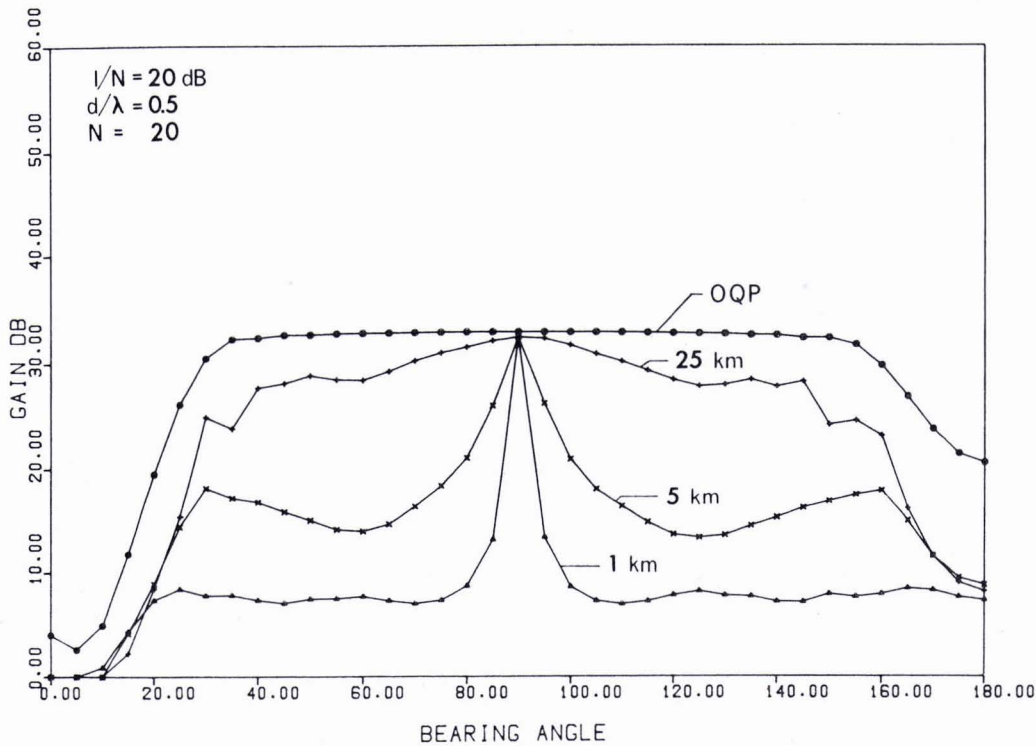

Fig. 9. Inclusion of signal in adaptation.

(a) In the shallow water sound propagation channel the sound energy of a point source may be spread over a vertical angle of roughly ±20°. The vertical energy spread appears to the horizontal array as a horizontal spread which is proportional to the cosine of the bearing, i.e. zero for broadside and ±20° for endfire. The results obtained in this paper are related to such a case.

(b) For small apertures (less than 20λ) linear adaptive processors (OLP, linear MBP) are almost optimum. For larger apertures quadratic beamforming must be applied.

(c) Cosine-shading is a useful approximation to optimum processing for about 40λ aperture (about 3 dB loss).

(d) Combining adjacent sensors to dipoles is a useful means for suppression of one point source with known direction.

(e) The adaptive multi-beam processor is the best sub-optimum array processor for arbitrary apertures (loss: about 1 dB).

(f) The signal spread causes adaptive systems to be very sensitive to inclusion of signal in adaptation (passive systems). Even the performance of constrained processors is degraded seriously because the constraint to be superimposed on adaptation depends considerably on the particular parameters of the medium.

Acknowledgement

List of symbols

a	source strength
A_n	modal amplitude
$A_n(i)$	range dependent modal amplitude at ith sensor
$A_n(r_0)$	modal amplitude at range r_0
α_n	modal attenuation coefficient
b	vector containing beamformer weights
b_i	ith beamformer vector
β	bearing angle
$c(z)$	sound velocity at depth z
c	interference vector
C	matrix of interference vectors
c_i	elements of c
d_i	range increments between array sensors
d	spacing of sensors
D	detection index
η	detection threshold
f	frequency
F	generalized beamformer matrix
G	gain
γ_n	modal arrival angle
h	vector of linear processor weights
H	beamformer matrix after pre-transform
H	water depth
I	unity matrix
j	$\sqrt{-1}$
k	$2\pi/\lambda$
k_0	$\omega/c(z)$
k_n	$2\pi/\lambda_n$, modal wavenumber
K	processor matrix
L	rank of pre-transform
λ	wavelength
M	number of modes
N	number of sensors
N	noise covariance matrix after pre-transform
n	noise and interference vector after pre-transform
ν	"noise"
O	null matrix
ω	$2\pi f$
P	signal covariance matrix
P_n	noise power
P_w	white noise power
P_s	signal power
$p(\cdot)$	pressure
ψ	output signal of processors
Q_I	covariance matrix of interference

$\mathbf{Q}$	covariance matrix of interference plus noise
r	range
r_0	range of first sensor
ρ_{il}	element of $\mathbf{Q}_I$ or $\mathbf{P}$
$\mathbf{R}$	suboptimum beamformer matrix
$\mathbf{S}$	signal covariance matrix after pre-transform
s	signal vector after pre-transform
σ	"signal"
$\sigma + \nu$	"signal + noise"
t	time
$\mathbf{T}$	pre-transform matrix
tr	trace of a square matrix
$u_n(\cdot)$	normal mode function
$\mathbf{W}$	noise suppression matrix
x	vector of received signals
x_i	elements of x
z	receiver depth
z_0	source depth
$*$	complex conjugate or complex conjugate transpose.

References

[1] F. Bryn, "Optimum signal processing of three-dimensional arrays operating on Gaussian signals and noise", *J. Acoust. Soc. Amer.*, Vol. 34, No. 3, 1962, pp. 289–297.

[2] H. Mermoz, "Filtrage adapté et utilisation optimal d'une antenne", *NATO Advanced Study Institute on Signal Processing* with Emphasis on Undertater Acoustics, Grenoble, France, 1964, pp. 160–299.

[3] H. Mermoz, "Antennes de détection optimales et adaptives", *Collection Technique et Scientifique du CNET*, 1971, Ed. Jaques et Demontrand, France (recueil d'articles parus de 1963 à 1970 dans les Anuales des Télécommunications).

[4] H. Cox, "Interrelated problems in detection and estimation", *NATO Advanced Study Institute on Signal Processing*, Enschede, 1968, pp. 23-1–23-66.

[5] H. Cox, "Sensitivity in adaptive beamforming", *NATO Advanced Study Institute on Signal Processing*, Academic Press, London and New York, 1973, pp. 619–645.

[6] B. Widrow, "Adaptive antenna systems", *Proc. I.E.E.E.*, Vol. 55, No. 12, 1967, pp. 2143–2159.

[7] W. Bühring and R. Klemm, "An adaptive filter for suppression of clutter with unknown spectrum" (in German), *Frequenz*, Vol. 30, No. 9, 1976, pp. 238–243.

[8] R. Klemm, "Adaptive clutter suppression in step scan radars", *I.E.E.E. Trans. A.E.S.*, Vol. 14, No. 1, 1976, pp. 685–688.

[9] R. Klemm, "Detection performance of horizontal linear hydrophone arrays in shallow water", *SACLANTCEN report*, 1980.

[10] F.B. Jensen and M.C. Ferla, "SNAP, the SACLANTCEN Normal Mode Acoustic Propagation Model", *SACLANTCEN SM-121*, 1979.

[11] W.A. Kuperman and F. Ingenito, "Attenuation of the coherent component of sound propagating in shallow water with rough boundaries", *J. Acoust. Soc. Amer.*, Vol. 61, No. 5, pp. 1178–1187, May 1977.

[12] C.S. Clay, "Effect of a slightly irregular boundary on the coherence of waveguide propagation", *J. Acoust. Soc. Amer.*, Vol. 36, 1964, pp. 833–837.

[13] C. Giraudon, "Results on active sonar optimum array processing", *NATO Advanced Study Institute on Signal Processing*, Academic Press, 1973, pp. 495–505.

[14] N.L. Owsley, "A recent trend in adaptive spatial processing for sensor arrays: Constrained adaptation", *NATO Advanced Study Institute on Signal Processing*, Academic Press, 1973, pp. 591–604.

[15] V.C. Anderson, "Dicanne, a realizable adaptive process", *J. Acoust. Soc. Amer.*, Vol. 41, No. 2, 1969, pp. 398–405.

[16] O.S. Halpeny and D.G. Childers, "Composite wavefront decomposition via multidimensional digital filtering of array data", *I.E.E.E. Trans. Circuits Systems*, Vol. CAS-22, 1975, pp. 552–563.

[17] I. Dyer, "Statistics of sound propagation in the ocean", *J. Acoust. Soc. Amer.*, Vol. 48, No. 1, 1970, pp. 337–345.

INITIAL DISTRIBUTION

MINISTRIES OF DEFENCE	Copies	SCNR FOR SACLANTCEN	Copies
MOD Belgium	2	SCNR Belgium	1
DND Canada	10	SCNR Canada	1
CHOD Denmark	8	SCNR Denmark	1
MOD France	8	SCNR Germany	1
MOD Germany	15	SCNR Greece	1
MOD Greece	11	SCNR Italy	1
MOD Italy	10	SCNR Netherlands	1
MOD Netherlands	12	SCNR Norway	1
CHOD Norway	10	SCNR Portugal	1
MOD Portugal	5	SCNR Turkey	1
MOD Turkey	5	SCNR U.K.	1
MOD U.K.	16	SCNR U.S.	2
SECDEF U.S.	61	SECGEN Rep. SCNR	1
		NAMILCOM Rep. SCNR	1

NATO AUTHORITIES		NATIONAL LIAISON OFFICERS	
Defence Planning Committee	3	NLO Canada	1
NAMILCOM	2	NLO Denmark	1
SACLANT	10	NLO Germany	1
SACLANTREPEUR	1	NLO Italy	1
CINCWESTLANT/COMOCEANLANT	1	NLO U.K.	1
COMIBERLANT	1	NLO U.S.	1
CINCEASTLANT	1		
COMSUBACLANT	1	NLR TO SACLANT	
COMMAIREASTLANT	1	NLR Belgium	1
SACEUR	2	NLR Canada	1
CINCNORTH	1	NLR Denmark	1
CINCSOUTH	1	NLR Germany	1
COMNAVSOUTH	1	NLR Greece	1
COMSTRIKFORSOUTH	1	NLR Italy	1
COMEDCENT	1	NLR Netherlands	1
COMMARAIRMED	1	NLR Norway	1
CINCHAN	1	NLR Portugal	1
		NLR Turkey	1
		NLR UK	1
		NLR US	1

	Copies
Total initial distribution	236
SACLANTCEN Library	10
Stock	34
Total number of copies	280